William R. Wiley
EMSL
Environmental Molecular Sciences Laboratory

EMSL Report

May/June 2006

The W.R. Wiley Environmental Molecular Sciences Laboratory (EMSL) is a U.S. Department of Energy (DOE) national scientific user facility located at Pacific Northwest National Laboratory (PNNL) in Richland, Washington. EMSL is operated by PNNL for the DOE Office of Biological and Environmental Research. At one location, EMSL offers a comprehensive array of leading-edge resources in six research facilities.

Access to the capabilities and instrumentation in EMSL facilities is obtained on a peer-reviewed proposal basis. Users are participants on accepted proposals. Staff members work with users to expedite access to the facilities and scientific expertise. The Bimonthly Report documents research and activities of EMSL staff and users.

Research Highlights

Evidence of Hollow Gold Cages

S Bulusu,[a] X Li,[b] LS Wang,[b] and XC Zeng[a]
(a) University of Nebraska, Lincoln, Nebraska
(b) Washington State University Tri-Cities, Richland, Washington

Clusters are small groups of atoms that often have different properties than their corresponding bulk materials. In this work, the researchers have found that some gold atom clusters form structures with hollow cages. The existence of these cages may allow for the insertion of other atoms to create new materials with unique properties for a wide range of applications.

The detection of carbon-free hollow cages has attracted much interest since the discovery and synthesis of the buckyball, C_{60}, and the higher fullerenes. Although "free-standing" inorganic cages have been synthesized, bare elemental metal cages have not been observed in nature or detected in the laboratory. Among metals, gold has unique properties, including strong relativistic effects and aurophilic attraction. Recently, a fullerene-like hollow cage with 32 gold atoms was predicted to be highly stable. However, photoelectron spectroscopy (PES) combined with theoretical calculations shows that at this relatively large size the overwhelming population of low-lying clusters for Au_{32} near room temperature appears to consist of only compact structures because of the entropic factor. Other, larger gold clusters with cage-like local minimum structures also have been suggested, but none have been observed experimentally. Conversely, it has been established from both ion-mobility and PES experiments that the most stable anion gold clusters (Au_n) in the size range n = 5–13 possess planar structures and

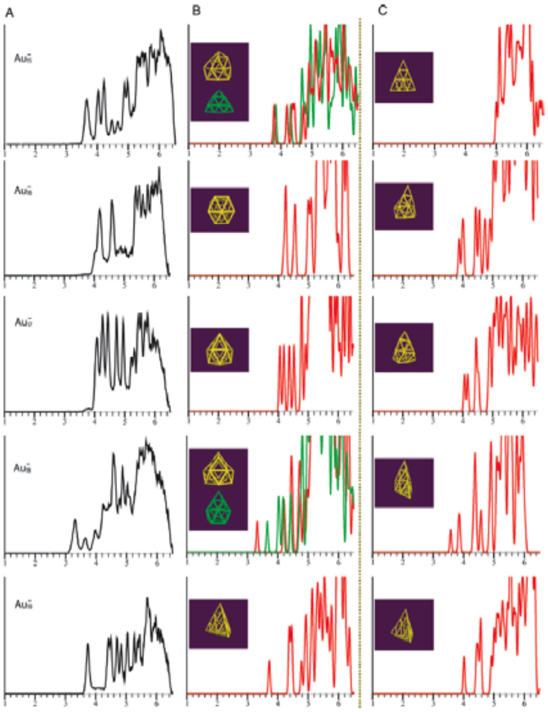

Figure 1. Experimental photoelectron spectra of Au_n^- (n = 15–19) compared with those simulated theoretically. (A) Experimental spectra measured at 193 nm (6.4 eV). (B) The simulated spectra for one (or two) lowest-lying isomer. (C) The simulated spectra for the non-hollow-cage candidate isomer.

that a structural transition from planar to three-dimensional structures occurs at n = 14. Beyond n = 14, previous global-minimum searches based on empirical potential functions of gold or semi-empirical tight-binding models of gold suggest that all low-lying isomers of gold clusters assume space-filling compact structures. Among the larger gold clusters, Au_{20} is the most interesting; it has been found to possess a pyramidal structure with tetrahedral symmetry just as carved out of the bulk face-centered cubic crystal.

To elucidate the structural transition from the planar Au at n = 13 to the pyramidal Au_{20}, we carried out a joint experimental PES and theoretical study on Au_n^- for n = 15–19. The measured spectra are shown in Figure 1A with numerous well-resolved features in the lower binding energy part, which are used to compare with theoretically simulated spectra (Figures 1B and 1C) with the candidate lowest-energy clusters.

Remarkably, we observed that all but a total of three candidate lowest-energy isomers of Au_{16}^- , Au_{17}^-, and Au_{18}^- are "hollow cages" with an empty interior space. The interior space (typically with length scale 5.5Å) of these hollow cages can easily host a foreign atom. Among the five candidate lowest-energy structures of Au_{15}^-, three are flat-cage structures, whereas the other two are pyramid-like structures. Previous studies have shown that in stable gold clusters, gold atoms tend to have a maximum coordination number of six (e.g., in the two-dimensional planar structures of Au_9 to Au_{13} and in the pyramidal structure of Au_{20}). Hence, it is understandable that both the flat-cage and pyramid-like structures are energetically competitive for the gold clusters within the size range Au_{14} to Au_{20}. Conversely, it is quite surprising that the hollow-cage structures dominate the low-lying population of Au_{16}^- to Au_{18}^- clusters. Specifically, at Au_{16}, only one of the five candidate lowest-energy structures has a flat-cage structure whose interior length scale can be 5Å The structural transition from hollow-cage to pyramid-like structure appears to occur at Au_{19}. To illustrate the structural evolution of gold clusters from two-dimensional planar to three-dimensional flat-cage, hollow-cage, and pyramid-like structures, we show in Figure 2 those candidate lowest-energy clusters that can provide a reasonable match to the experimental photoelectron spectra (Figures 1A and B). Our first-principles global search provides the electronic energy based evidence that the overwhelming majority of the low-lying clusters of Au_{16}^- to Au_{18}^- exhibit hollow-cage structures. These clusters and their larger neighbors are stable at room temperature; the size of the hollow should allow for other atoms to be trapped inside. The interior doping of these hollow clusters may dramatically change the cluster properties and thereby allow for the tailoring of the clusters for specific applications. This work was featured on the cover of the May 23, 2006, issue of the *Proceedings of the National Academy of Science* (Figure 3) (Bulusu et al. 2006).

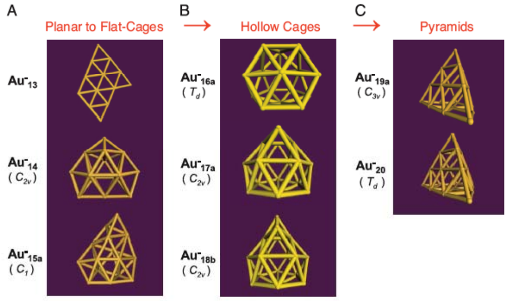

Figure 2. Structural evolution of mid-sized gold anion clusters from Au_{13} to Au_{20}. (A) The two-dimensional planar to three-dimensional flat-cage structural transitions (11). (B) The hollow gold cages with diameters 5.5 Å. (C) The pyramid-like clusters, which resemble bulk gold.


PNAS

Hollow gold nanocages

Figure 3. May 23, 2006, issue of the *Proceedings of the National Academy of Science.*

Citation

Bulusu S, X Li, LS Wang, and XC Zeng. 2006. "Evidence of Hollow Golden Cages." *Proceedings of the National Academy of Science* 103(22):8326-8330.

A Review of Multidimensional, Multifluid Intermediate-Scale Experiments: Nonaqueous Phase Liquid Dissolution and Enhanced Remediation

M Oostrom,[a] JH Dane,[b] and TW Wietsma[c]

(a) Pacific Northwest National Laboratory, Richland, Washington
(b) Auburn University, Auburn, Alabama
(c) W.R. Wiley Environmental Molecular Sciences Laboratory, Richland, Washington

Intermediate-scale flow cell experiments are used to simulate field-scale processes in the laboratory under controlled conditions.

An invited review of multidimensional, multifluid, intermediate-scale experiments involving nonaqueous phase liquids (NAPLs) was recently published in *Vadose Zone Journal* (Oostrom et al. 2006). These experiments were conducted at an intermediate scale between column studies and field trials (Figure 1). The primary advantage of intermediate-scale flow cell experiments is that field-scale processes can be simulated under controlled conditions. The experiments are frequently conducted to provide datasets to test and verify numerical and analytical flow and transport models. The controlled setting and laboratory instrumentation reduces the uncertainty in parameter estimation, allowing comparisons between simulation and experimental results to focus on flow and transport processes. A total of about 125 original contributions were identified and reviewed.

Figure 1. EMSL researchers test theories of flow and transport. The study coupled processes involved with microbial, reactive chemical, NAPLs, colloid transport, or test subsurface remediation scenarios using the Subsurface Flow and Transport Laboratory.

Research needs in NAPL dissolution include:

- Long-term dissolution studies of multicomponent NAPL in heterogeneous porous media
- Increased understanding of NAPL dissolution upscaling from the pore scale to the field scale
- New theoretical models for NAPL dissolution in mixed-wet porous media.

Research needs in NAPL remediation include:

- Development of multi-flood techniques that combine alcohol and surfactant flushing
- New dense-brine injection techniques
- Development of neutral buoyancy techniques for application in heterogeneous porous media
- Application of heat-based remediation techniques.

Citation

Oostrom M, JH Dane, and TW Wietsma. 2006. “A Review of Multidimensional, Multifluid Intermediate-Scale Experiments: Nonaqueous Phase Liquid Dissolution and Enhanced Remediation.” *Vadose Zone Journal* 5:570-598. doi:10.2136/vzj2005.0125

A Solid-State ^{95}Mo NMR and Computational Investigation of Dodecahedral and Square Antiprismatic Octacyanomolybdate(IV) Anions: Is the Point-Charge Approximation an Accurate Probe of Local Symmetry?

MAM Forgeron[(a)] and RE Wasylishen[(a)]
(a) University of Alberta, Edmonton, Alberta, Canada

Solid-state nuclear magnetic resonance (NMR) studies of low-gamma nuclei have been hampered in the past because of inherent difficulties associated with observing low-frequency quadrupolar nuclei. Such studies are becoming feasible and productive with the use of the highest possible magnetic field strengths coupled with sensitivity-enhancement experiments.

Because of the experimental challenges they present, solid-state NMR studies of quadrupolar nuclei with small magnetic moments represent a relatively undeveloped area of research. The inherently low NMR sensitivity of such nuclei means that considerable time is required to obtain NMR spectra of adequate signal-to-noise characteristics—a problem that is often compounded by the fact that solid-state NMR spectra, particularly of quadrupolar nuclei, may span several hundred kilohertz. Recent technological advances have enabled NMR data collection for challenging quadrupolar nuclei that have previously been refractory to observation. For example, the development of high-field magnets and new-and-improved pulse sequences facilitate data collection; high magnetic fields result in increased sensitivity and amplification of the magnetic shielding, σ, interaction and, in addition, substantially reduce probe ringing, which is often an experimental hindrance when observing low-frequency quadrupolar nuclei. New pulse sequences include a variety of sensitivity-enhancement techniques that further improve the quality of the NMR experiment and result in significant reductions in experimental time.

One important isotope that falls into the small magnetic moment category is ^{95}Mo. Despite the prevalence of molybdenum in modern chemistry, ^{95}Mo has received little attention from the solid-state NMR community, primarily because of its unfavorable properties: $\Xi = 6.547$ MHz, N.A. = 15.92 %, $Q = -0.022 \times 10^{-28}$ m^2. Unfortunately, the small quadrupole moment, Q, of ^{95}Mo creates an additional impediment for NMR studies in the solid state to long spin-lattice relaxation times. Nevertheless, by employing the highest possible magnetic field strengths and available sensitivity-enhancement techniques, we have been able to undertake ^{95}Mo NMR studies. Through determination of the molybdenum σ and electric field gradient (EFG) tensors, a wealth of information on molecular and electronic structure can be obtained.

In this study, we have demonstrated the efficiency and effectiveness of solid-state ^{95}Mo NMR spectroscopy as a tool for analyzing two symmetry forms of the diamagnetic octacyanomolybdate(IV) anion: 1) the approximate dodecahedral, D_{2d}, symmetry and 2) the approximate square antiprismatic, D_{4d}, symmetry. The success of this study is attributed to the use of the highest available magnetic field strengths, 21.15 tesla (T), which corresponds to 900-MHz proton frequency; 17.63 T (750 MHz); and 11.75 T (500 MHz), and the quadrupolar Carr-Purcell Meiboom-Gill (QCPMG) and double-frequency sweep (DFS)/QCPMG sensitivity-enhancement techniques. By examining the D_{2d} and D_{4d} $Mo(CN)_8^{4-}$ anions in the solid state, we have studied each structure independently and have characterized the molybdenum σ and EFG interactions, thereby avoiding problems associated with solution NMR studies, such as ligand exchange or interconversion between symmetry forms. The acute sensitivity of the molybdenum σ and EFG tensors to small changes in the local structure of these anions has allowed the approximate D_{2d} and D_{4d} $Mo(CN)_8^{4-}$ anions to be readily distinguished.

Our results indicate that the magnitudes of the molybdenum σ and EFG interactions are comparable for the D_{2d} and D_{4d} $Mo(CN)_8^{4-}$ anions; however, the relative values and orientations of the principal components of the molybdenum σ and EFG tensors for the two symmetry forms are different, resulting in ^{95}Mo NMR line shapes that are distinctly different at the fields employed here (Figure 1). Quantum chemical calculations of the molybdenum σ and EFG tensors, using zeroth-order regular approximation density functional theory (ZORA DFT) and restricted Hartree-Fock (RHF) methods, have also been carried out, and the results obtained are in good agreement with experimental results. The most significant and surprising result from the DFT and RHF calculations is a substantial EFG at molybdenum for an isolated $Mo(CN)_8^{4-}$ anion possessing an ideal square anti-prismatic structure; this is contrary to the point-charge approximation, which predicts a zero EFG at molybdenum for this structure.

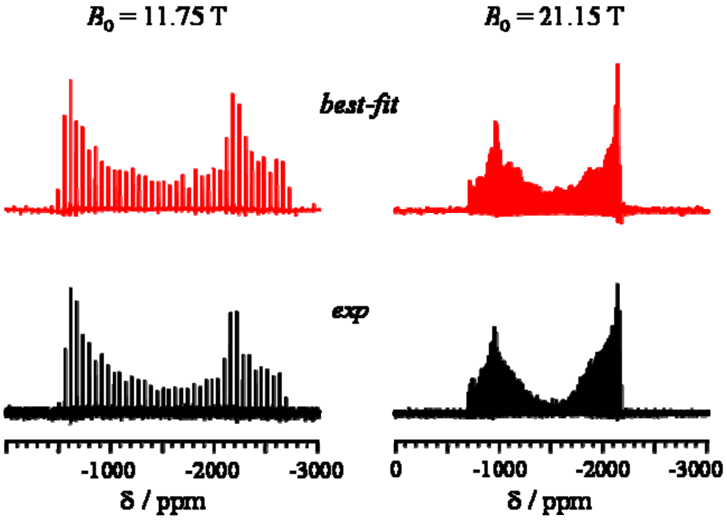

Figure 1. Experimental and best-fit simulated ^{95}Mo central-transition NMR spectra of a solid, stationary sample of $Tl_4Mo(CN)_8$ acquired using the QCPMG pulse sequence at 11.75 T (left) and the DFS/QCPMG pulse sequence at 21.15 T (right). A total of 31 760 transients were summed for $Tl_4Mo(CN)_8$ at 11.75 T and 8192 at 21.15 T.

Citation

Forgeron MAM and RE Wasylishen. 2006. "A Solid-State ^{95}Mo NMR and Computational Investigation of Dodecahedral and Square Antiprismatic Octacyanomolybdate(IV) Anions: Is the Point-Charge Approximation an Accurate Probe of Local Symmetry?" *Journal of the American Chemical Society* 128:7817-7827.

Identification and Post-Translational Modification of Mitotic Regulatory Proteins

F Yang,[a] MA Gritsenko,[a] DG Camp,[a] RD Smith,[a] and DL. Stenoien[a]
(a) Pacific Northwest National Laboratory, Richland, Washington

This highlight focuses on a class of proteins known as chromosomal passengers (CP) that, because of their complex localization patterns, are thought to play multiple roles in cell proliferation and cell cycle checkpoint signaling pathways. Therefore, the study of CPs represents an area of intense research because of their importance as mitotic regulators and their potential to be cancer targets. Transient protein modification by phosphorylation plays an essential role in regulating mitosis and preventing cancer. This research is designed to identify novel phosphoproteins and post-translational modifications that regulate mitotic progression.

Spatial and temporal changes in protein localization play important roles in regulating protein activity in many cellular processes. This is most evident during mitosis when cells undergo dramatic changes in their architecture. Phosphorylation of critical mitotic regulatory proteins is recognized as a key mechanism that controls the successful completion of mitosis with the high fidelity needed to prevent aneuploidy and possible cancer development. In our studies, we have chosen to perform targeted proteomic analyses on a subset of enriched mitotic regulatory proteins to increase the detection of very low abundance protein complexes and their post-translational modifications. We are using a phosphorylation site-specific antibody (P190) that recognizes several mitotic phosphoproteins that behave as CPs. CPs undergo dramatic changes in their localization as cells progress through mitosis, localizing on kinetochores during prophase and metaphase and at the mid-zone and mid-body at later stages of mitosis (Figure 1). Many of the known CPs, including aurora-B kinase, play critical regulatory roles during mitosis, and their functions are often compromised during cancer development.

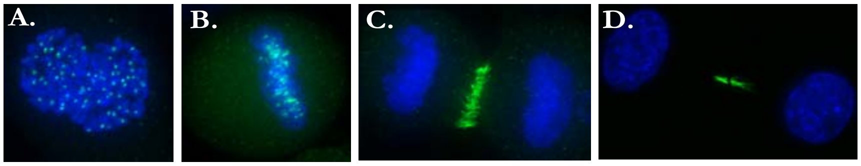

Figure 1. The P190 antibody recognizes chromosomal passenger proteins. Kinetochores are immunoreactive for the P190 antibody (green) in prophase (A) and remain labeled through metaphase (B). As the chromosomes (blue) separate, P190 labels the mid-zone during anaphase (C) and the mid-body after cell division (D).

To identify the phosphoproteins, protein complexes, and phosphorylation sites bound by the P190 antibody, we employed several mass spectrometry-based approaches to identify both peptides and phosphopeptides present in P190 immunoprecipitates (IP) (Figure 2). In one approach, we performed mass spectrometry on protein IPs from mitotic cell lysates to identify the protein complexes recognized by the P190 antibody. Using this approach, we were able to identify 298 unique proteins in the P190 IP versus 41 unique proteins in the control IP. Several known CPs were specifically present in the P190 IP, including Aurora-B, RCC1-like/TD-60, and INCENP, all of which are present in the same protein complex. We also identified other proteins that have known roles in mitosis and/or localize to the mitotic apparatus. These proteins include Aurora-A, ch-TOG, cyclin B, NuMA, cytoplasmic dynein, tubulins, actin, and actin-binding proteins. Other identified proteins include those involved in various signaling pathways that regulate mitosis such as SMAD2, Casein Kinase 1, serine/threonine protein phosphatase 2A, ALPHA-1 CATENIN, and 14-3-3 proteins. Many of the proteins specifically present in the P190 IP include those proteins present in ribosomes and spliceosomes, large protein structures that have known but poorly understood functions during mitosis. We also identified a large number of hypothetical proteins and proteins with no clearly defined cellular functions that represent candidates for novel CPs.

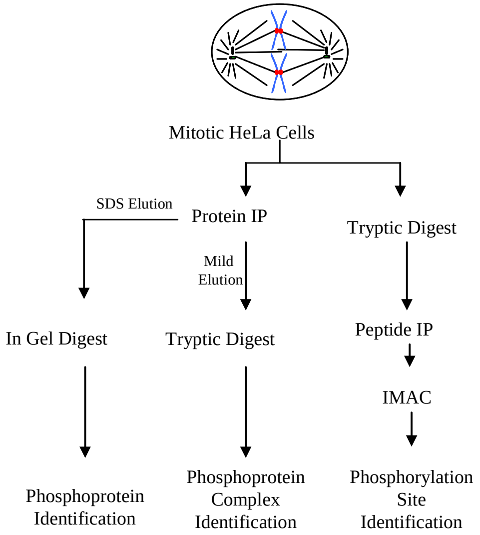

Figure 2. Strategy for identifying protein complexes and phosphorylation sites containing the P190 phosphoepitope.

The P190 antibody was generated using a phosphopeptide (VLPRGL[pS]PARQLL) uniquely present in the progesterone receptor. Because the antibody cross-reacts with other phosphoproteins, we reason that the antibody only reacts with a subset of the amino acids present in the phosphopeptide that may also be present in other proteins. To determine the critical amino acid residues recognized by the antibody, we performed a tryptic digest of mitotic cell lysates followed by a phosphopeptide IP, IMAC enrichment, and identification of phosphopeptides. The most abundant peptide from this analysis was derived from ribosomal protein L12 and had the sequence, K.IGPLGL[pS]PK.K). Other proteins present in both the phosphopeptide and protein IPs include ch-TOG (KAPGL[pS][pS]KAK), Otthump22591 (QPPLSL[pS]PAP), and Ric 8/synembrin (IQPMGM[pS]PRG).

From these peptides and the original starting peptide, we identified a motif of PXXLSP as the preferred binding motif of the P190 antibody. Interestingly, this motif is present in INCENP (PL**P**RT**L[pS]P**TP), the chromosomal passenger protein identified in the P190 protein IP. Other proteins in the protein IP containing this motif include SMAD2, stathmin 3, ABLIM1, Bcl9, Mystique, CAMTA1, Hira, and hypothetical protein DKFZP434K1815. Analysis of phosphorylation site databases showed that the motifs present in INCENP, SMAD2, stathmin 3, and ABLIM1 are phosphorylated *in vivo*. Functional assays are underway to address the significance of these specific phosphorylation events in regulating mitotic progression.

Identification of Isotopically Primitive Interplanetary Dust Particles

C Floss,[(a)] FJ Stadermann,[(a)] JP Bradley,[(b)] ZR Dai,[(b)] S Bajt,[(b)] G Graham,[(b)] and SA Lea[(c)]
(a) Washington University, St. Louis, Missouri
(b) Institute for Geophysics and Planetary Physics, Livermore, California
(c) W.R. Wiley Environmental Molecular Sciences Laboratory, Richland, Washington

Interplanetary dust particles (IDPs), which originate largely from comets and asteroids, are complex assemblages of various primitive solar system materials. Chondritic porous IDPs are dominated by anhydrous minerals, in contrast to chondritic smooth IDPs that are composed predominantly of hydrated layer lattice silicates. While specific parent bodies are not known, hydrated IDPs have been linked to asteroidal origins, whereas anhydrous IDPs may be more likely to have cometary origins.

Isotopic measurements of IDPs show the presence of abundant extra-solar phases. Significant depletions and enrichments in hydrogen isotopic compositions have been found in IDPs and almost certainly have an interstellar origin. The origin of nitrogen isotopic anomalies is more complicated than that of hydrogen, because nitrogen isotopic fractionation has not been observed in the interstellar medium and anomalous nitrogen can also have a nucleo-synthetic origin. However, recent theoretical work shows that chemical reactions in dense molecular clouds can produce elevated $^{15}N/^{14}N$ ratios.

High spatial resolution surface analytical instrumentation such as NanoSIMS and scanning auger microscopy have the ability to make isotopic measurements and identify mineralogical phases at the sub-micron scale, providing renewed opportunities to investigate the compositions of IDPs. Our goal has been to gain a better understanding of the abundance, nature, and distribution of isotopically anomalous phases in IDPs and, thereby, constrain both the nature of these phases and the parent bodies from which IDPs originate.

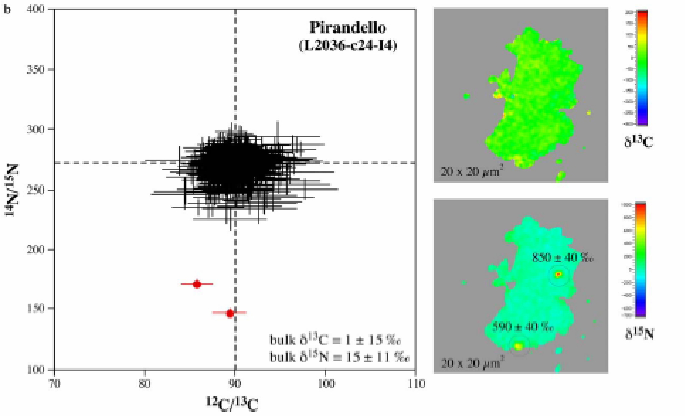

Figure 1. Carbon and nitrogen isotopic compositions of Pirandello from NanoSIMS analysis. Shown are isotope plots of the $^{12}C/^{13}C$ and $^{14}N/^{15}N$ ratios of 500 nm-sized subregions of the IDPs and false color images of the $\delta^{13}C$ and $\delta^{15}N$ compositions of the particles. Pirandello has isotopically normal bulk compositions in carbon and nitrogen, but contains two hot spots enriched in ^{15}N. Dashed lines show terrestrial carbon and nitrogen ratios.

Carbon and nitrogen isotopic compositions were measured in 39 IDPs from NASA collector flags L2009, L2011, and L2036. Hydrogen isotopic compositions were measured in a subset of these 39 IDPs. Typical data collected from these 39 IDPs, using NanoSIMs imaging and scanning Auger microscopy, are shown in Figure 1.

Auger elemental maps of pre-solar grain D1 from the IDP Deledda show that it is an iron-rich silicate (Figure 2). Iron-magnesium silicates, such as olivine and pyroxene, are expected to have magnesium-rich compositions under conditions of equilibrium condensation in the stellar winds of oxygen-rich RGB and AGB stars. Deledda appears to be an anhydrous IDP, which is unlikely to have experienced significant secondary processing. Thus, the pre-solar grain D1 may represent a primary iron-rich silicate condensate that formed under nonequilibrium conditions.

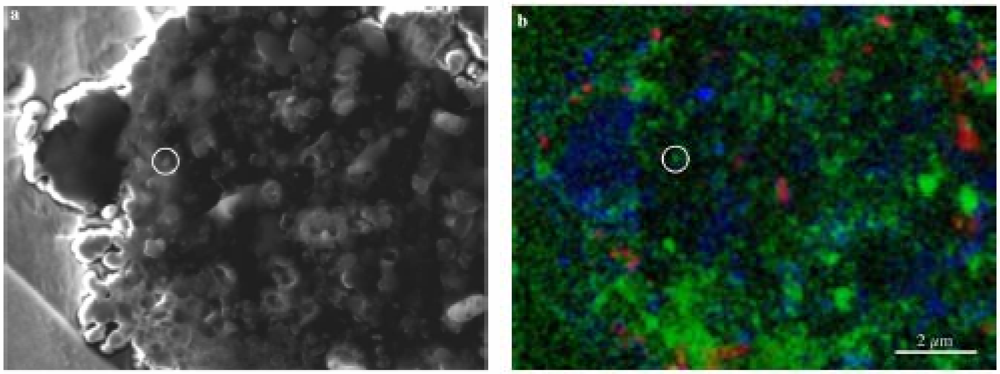

Figure 2. Auger elemental maps of presolar grain D1 from the IDP Deledda.

Isotopic imaging of a suite of IDPs shows that nitrogen isotopic compositions can be used to characterize IDPs and identify those that share a variety of primitive isotopic compositions, including the presence of abundant pre-solar silicate grains (Floss et al. 2006). Hydrogen and nitrogen isotopic compositions in these IDPs show similar distributions; fractionations are present both as small D-rich or ^{15}N-rich hot spots and as larger more diffuse anomalous regions. However, hydrogen and nitrogen anomalies are not correlated and D enrichments are not preferentially associated with isotopically primitive IDPs. Pre-solar silicate grains in the IDPs show a variety of isotopic compositions that are similar to the oxygen isotopic compositions of pre-solar silicate and oxide grains from primitive meteorites. Most of the grains have isotopic ratios consistent with origins from red giant or asymptotic giant branch stars. Pre-solar silicate abundances in the isotopically primitive IDPs are significantly higher than in most primitive meteorites, a characteristic that emphasizes the primitive nature of IDPs.

Citation

Floss C, FJ Stadermann, JP Bradley, ZR Dai, S Bajt, G Graham, and AS Lea. 2006. "Identification of Isotopically Primitive Interplanetary Dust Particles: A NanoSIMS Isotopic Imaging Study." *Geochimica et Cosmochimica Acta* 70:2371-2399.

Full Collection of More Than 1.6 Million Proteins Analyzed Using ScalaBLAST

***CS Oehmen*[a] *and P Hugenholtz*[b]**
(a) Pacific Northwest National Laboratory, Richland, Washington
(b) Lawrence Berkeley National Laboratory, Berkeley, California

ScalaBLAST is a high-throughput sequence analysis engine based on the National Center for Biotechnology Information BLAST distribution. It allows users to harness the power of supercomputers or commodity clusters to accelerate the rate of performing normal BLAST searches against a target database.

One of the key limitations in any sequence analysis pipeline is the need to compare a large collection of proteins from many organisms against itself to detect commonalities between the proteins of different species and within a species. In conjunction with the Joint Genome Institute, current steward of a large collection of microbial genomes, CS Oehmen of Pacific Northwest National Laboratory and P Hugenholtz of Lawrence Berkeley National Laboratory used ScalaBLAST to analyze the full collection of more than 1.6 million proteins against itself in less than 13 hours using 1000 processors of the MPP2 supercomputer in the EMSL Molecular Science Computing Facility (MSCF).

An additional large search was performed in which each of the 1.6 million microbial protein sequences was compared to the nonredundant list of more than 3 million proteins distributed by the National Center for Biotechnology Information. This step is often performed on genomes as part of a quality control process. For a dataset of this size, it is not possible for most BLAST users to analyze the full dataset in a tractible time, because for most standalone BLAST installations, a single genome of a few thousand proteins takes many days to process.

Oehmen and Hugenholtz were able to use ScalaBLAST on MPP2 to process the entire list of 1.6 million proteins against the nonredundant database using 1500 processors in fewer than 20 hours. This collection of results will be shared with the Joint Genome Institute to be used in conjunction with the microbial genome data as a significant information resource for the worldwide community of biological researchers.

Full Stannaspherene: A Highly Symmetric Cage of Sn_{12}^{2-} Dianion

L-F Cui,(a,b) X Huang,(a,b) LM Wang,(a,b) DY Zubarev,(d) AI Boldyrev,(d) J Li,(c) and LS Wang(a,b)
(a) Washington State University Tri-Cities, Richland, Washington
(b) Pacific Northwest National Laboratory, Richland, Washington
(c) W.R. Wiley Environmental Molecular Sciences Laboratory, Richland, Washington
(d) Utah State University, Logan, Utah

In an effort to understand the semiconductor-to-metal transition in main-group elemental clusters, photoelectron spectroscopy (PES) was used to observe a remarkably stable tin cluster. The spectrum of Sn_{12}^- *is remarkably simple and totally different from the corresponding* Ge_{12}^- *cluster, suggesting that* Sn_{12}^- *is a unique and highly symmetric cluster.*

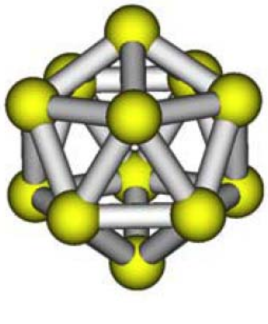

Figure 1. Computationally optimized structures of icosahedral Sn_{12}^- cluster.

Theoretical analysis and computational calculations show that the neutral Sn_{12}^- monoanion cluster has a slightly distorted icosahedral cage with C_{5v} symmetry (Figure 1). Adding an electron to Sn_{12}^- results in a stable closed-shell icosahedral I_h-Sn_{12}^{2-} cluster, which was synthesized in the form of KSn_{12-} ($K^+[Sn_{12}^{2-}]$) with a similar PES spectrum as Sn_{12}^-. The calculated energy gap between the highest occupied and lowest unoccupied orbitals in the I_h-Sn_{12}^{2-} is 1.9 eV, which is even larger than that in C_{60} (1.62 eV), providing further evidence for its high stability. The theoretically calculated energy levels, including spin-orbit coupling effects, are in good agreement with the experimentally observed spectra. The I_h-Sn_{12}^{2-} cage is shown to be bonded by four delocalized radial π bonds and nine delocalized on-sphere tangential σ bonds from the 5p orbitals of the tin atoms, whereas the $5s^2$ electrons remain largely localized and nonbonding. The bonding pattern in Sn_{12}^{2-} is similar to the well-known aromatic $B_{12}H_{12}^{2-}$ cage, with the 12 $5s^2$ localized electron pairs replacing the 12 B-H bonds. Because of the delocalized π bonding in Sn_{12}^{2-} and its spherical symmetry, the name "stannaspherene" is suggested for this highly stable species.

While cage structures involving tin were known in inorganic complexes and the Zintl phases, the I_h-Sn_{12}^{2-} cage was unknown. The high stability of this cluster suggests that it may be synthesized in the solid state using suitable ligands or counter ions. More interestingly, the Sn_{12}^{2-} cage has a diameter of ~6.1Å, which is only slightly smaller than that of C_{60}, and it can host an atom inside much like the endohedral fullerenes. Preliminary experimental and theoretical results suggest that most transition metal atoms can be hosted inside the Sn_{12}^{2-} cage, yielding a large class of novel endohedral stannaspherene. These metal-encapsulated stannaspherene clusters give rise to a large family of endohedral chemical building blocks for cluster-assembled nanomaterials. This work is published in the Journal *of the American Chemical Society* (Cui et al. 2006).

Citation

Cui L-F, X Huang, LM Wang, DY Zubarev, AI Boldyrev, J Li, and LS Wang. 2006. "Sn_{12}^{2-}: Stannaspherene." *Journal of the American Chemical Society* 128(26):8390-8391.

Computer Simulation of Radiation Effects in Zircon

R Devanathan,[a] LR Corrales,[a] WJ Weber,[a] A Chartier,[b] and C Meis[b]
(a) Pacific Northwest National Laboratory, Richland, Washington
(b) INSTN/UEPEM CEA-Saclay, Gif-Sur-Yvette, France

Using the computational resources of the MSCF MPP2 supercomputer and the NWfs (Northwest file system), massively parallel molecular dynamics simulations of uranium recoil damage in zircon were performed. Zircon is a durable ceramic that is a promising candidate for the safe immobilization of excess weapons-grade plutonium and high-level nuclear waste.

When doped with actinides, zircon undergoes α-decay that produces 70- to 100-keV heavy ion recoil. The recoil dissipates its energy by a cascade of atomic collisions, leading to defect production at the atomic-level, loss of crystalline structure, significant increase in leach rate of actinides, and degradation of mechanical properties. Because of the short time (ps) and length (nm) scales over which these processes take place, they are not easily accessed by experiments. To understand the fundamentals of radiation damage in ceramics and to design better nuclear waste forms, realistic computer simulations are needed in conjunction with experiments to shed light on the dynamics of collision cascades.

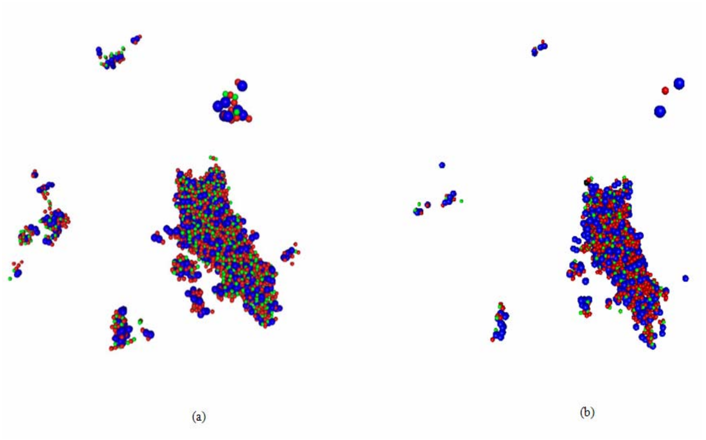

Figure 1. 30-keV uranium cascade in zircon showing (a) defects and (b) amorphous regions. The elements zirconium, silicon, and oxygen are represented by green, blue, and red, respectively.

In this project, the researchers simulated 10- and 30-keV uranium recoils in zircon, and developed new algorithms to distinguish between perfect crystalline, defective crystalline, and amorphous regions in the resulting collision cascade. The simulation cell contained more than one million atoms, which is remarkable in view of the long range of the Coulombic potential. Figure 1 shows the defects (a) and the amorphous regions produced by a 30-keV uranium recoil in zircon (b). The figure shows the formation of small amorphous clusters around the central amorphous core and nanoscale phase separation into zirconium- and silicon-rich regions. The observation of small nanosized amorphous clusters and segregation at the nanoscale enhances our under-standing of defect production in collision cascades in ceramics and provides useful information to guide the design of ceramic waste forms for nuclear waste disposal.

Awards and Recognition

Administrators Honored. NB Avery, PNNL Fundamental Science Directorate, and CC Montgomery, EMSL, were among the 26 nominees for the PNNL Administrator of the Year for 2006. This year's three honorees were Avery and TL Hoyem, Fundamental Science Directorate, and DF Mahon, Environmental Technology Directorate, with Hoyem receiving the Administrator of the Year award.

2005 M.T. Thomas Award Winner Announced. SN Kerisit was selected as the 2005 recipient of the M.T. Thomas Award for Outstanding Postdoctoral Achievement in recognition of such accomplishments as seminal and novel theoretical advancements in understanding electron transfer reactions at environmental interfaces and the impact on the field of geochemistry. Use of his unique combination of molecular dynamics simulations, electronic structure calculations, and kinetic Monte Carlo simulations constitutes the first attempt to computationally model the bioreduction of iron at mineral surfaces at the atomic level. Kerisit has used these techniques to contribute significantly to the EMSL Biogeochemistry Grand Challenge, where he has computed rates of electron transfer in iron oxide lattices and from heme groups in outer-membrane cytochromes to various hematite (α-Fe_2O_3) surfaces. His work has been published in the *Journal of Chemical Physics* and *Geochimica et Cosmochemica Acta.*

SN Kerisit, winner of the 2005 M.T. Thomas Award for Outstanding Postdoctoral Achievement.

Major Facility Upgrades

Spokane Cluster Now Operational. In May 2006, the Spokane Cluster replaced the Seattle Cluster, which consisted of networked Linux PCs used primarily for computational molecular modeling by and for users of the Environmental Spectroscopy and Biogeochemistry (ES&B) Facility. The new Spokane Cluster fills a critical computational need for ES&B Facility users because historically many of their projects have involved small molecules for which large-scale computing resources, such as the MPP2 supercomputer, are not required. The scientific systems under study emphasize environmental remediation, including electron transfer that involves metal oxides and metal complexes, reactions that involve halogenated organic molecules, and reactions at mineral surfaces. The Seattle Cluster enabled users to run the many small-scale, single-CPU jobs that were needed to address these ES&B Facility-specific topics. Although it is a "behind-the-scenes" piece of equipment and, therefore, is sometimes overlooked, the Seattle Cluster was the single most heavily used resource in the ES&B Facility.

For $100,000, the new 32-node (64-processor) Spokane Cluster was purchased to replace the Seattle Cluster. Each node consists of dual 3.0-GHz Intel EM64T Xeon processors, 4 Gb of memory, and 73 Gb of disk storage. This acquisition was the most cost-effective solution for maintaining the computational cycles required by many of the ES&B Facility users. The 64-processor machine equates to an overall computational power of 384 Giga-flops, which amounts to about $260 per Gigaflop. This is by far more cost effective than acquiring any other system, in part because the support infrastructure already is in place.

Visitors and Users

During this reporting period, a total of 322 users benefited from EMSL capabilities and expertise. This total included 187 onsite users and 135 remote users.

New EMSL Staff

Y Liu joined the Chemistry and Physics of Complex Systems Facility as a postdoctoral associate. He received his Ph.D. in atmospheric chemistry from the University of Michigan.

M Newburn joined the Chemistry and Physics of Complex Systems Facility as a post bachelor's degree limited term employee. He received his B.S. degree in electrical engineering from Walla Walla College.

JV Ortega joined the Chemistry and Physics of Complex Systems Facility as a postdoctoral associate. He received his Ph.D. in Atmospheric and Oceanic Sciences from the University of Colorado.

KA Glass was hired as a scientist in the MSCF's High Performance Software Development group for his technical expertise in parallel computing systems and his extensive teaching experience. Prior to joining EMSL, he was an Adjunct Assistant Professor of Computer Science at the University of Oregon.

JF Carr was hired as a Scientist in the MSCF's High Performance Computing & Network Services group. He received a B.S. in both mathematics and computer science from Walla Walla College.

Publications

Apra E, R Ferrando, and A Fortunelli. 2006. "Density-Functional Global Optimization of Gold Nanoclusters." *Physical Review B. Condensed Matter* 73(20):205414 -1 - 205414-5.

Armstrong RC, GK Kumfert, LC McInnes, SG Parker, BA Allan, S Matt, TG Epperly, and TL Dahlgren. 2006. "The CCa Component Model for High-Performance Scientific Computing." *Concurrency and Computation. Practice & Experience* 18(2):215-229.

Bayard E, S Hamel, and A Rochefort. 2006. "Hydrogen Bonding and Pi-Stacking in Highly Organized Arenes-Based Molecular Wire." *Organic Electronics* 7(3):144-154.

Bryantsev V and BP Hay. 2006. "Conformational Preferences and Internal Rotation in Alkyl- and Phenyl-Substituted Thiourea Derivatives." *Journal of Physical Chemistry A* 110(14):4678-4688.

Bulusu S, X Li, LS Wang, and X Zeng. 2006. "Evidence of Hollow Golden Cages." *Proceedings of the National Academy of Sciences* 103(22):8326-8330.

Bylaska EJ, K Tsemekhman, and F Gao. 2006. "New Development of Self-Interaction Corrected DFT for Extended Systems Applied to the Calculation of Native Defects in 3C-SiC." *Physica Scripta* T124:86-90.

Chekmenev EY, SM Jones, Y Nikolayeva, B Vollmar, TJ Wagner, PL Gorkov, WW Brey, MN Manion, KC Daugherty, and M Cotten. 2006. "High-Field NMR Studies of Molecular Recognition and Structure-Function Relationships in Antimicrobial Piscidins at the Water-Lipid Bilayer Interface." *Journal of the American Chemical Society* 128(16):5308-5309.

Chen W, G Huang, HB Lu, DE McCready, AG Joly, and JO Bovin. 2006. "Utilizing Nanofabrication to Construct Strong, Luminescent Materials." *Nanotechnology* 17(10):2595-2601.

Cui L, X Huang, LM Wang, DY Zubarev, AI Boldyrev, J Li, and LS Wang. 2006. "Sn_{12}^{2-}: Stannaspherene." *Journal of the American Chemical Society* 128:8390-8391.

Du S, J Francisco, GK Schenter, TD Iordanov, BC Garrett, M Dupuis, and J Li. 2006. "The OH Radical-H_2O Molecular Interaction Potential." *Journal of Chemical Physics* 124:224318-1 - 22418-15.

Elliott DC, GG Neuenschwander, TR Hart, J Hu, AE Solana, and C Cao. 2006. "Hydrogenation of Bio-Oil for Chemicals and Fuels Production." In *Science in Thermal and Chemical Biomass Conversion*, Vol. 2, AV Bridgwater and DGB Boocock, eds., pp. 1536-1546, CPL Press, Newbury, Berkshire, Great Britain.

Flaud JM, WJ Lafferty, RL Sams, and SW Sharpe. 2006. "High Resolution Spectroscopy of (H_2CO)-C-12-O-16 in the 1.9 to 2.56 mu m Spectral Range." *Molecular Physics* 102(12):1891-1903.

Forgeron MAM and RE Wasylishen. 2006. "A Solid-State 95Mo NMR and Computational Investigation of Dodecahedral and Square Antiprismatic Octacyanomolybdate(IV) Anions: Is the Point-Charge Approximation an Accurate Probe of Local Symmetry?" *Journal of the American Chemical Society* 128(24):7817-7827.

Gao F, R Devanathan, Y Zhang, M Posselt, and WJ Weber. 2006. "Atomic-Level Simulation of Epitaxial Recrystallization and Phase Transformation in SiC." *Journal of Materials Research 21*(6):1420-1426. doi:10.1557/JMR.2006.0176

Haynes PD, C Skylaris, AA Mostofi, and M Payne. 2006. "Elimination of Basis Set Superposition Error in Linear-Scaling Density-Functional Calculations with Local Orbitals Optimised *In Situ*." *Chemical Physics Letters* 422(4-6):345-349.

Kim D, J Szanyi, J Kwak, T Szailer, J Hanson, CM Wang, and CH Peden. 2006. "Effect of Barium Loading on the Desulfation of Pt-BaO/Al2O3 Studied by H2 TPRX, TEM, Sulfur K-edge XANES, and *In Situ* TR-XRD." *Journal of Physical Chemistry B* 110(21):10441-10448. doi:10.1021/jp060119f

Kirkpatrick R, T Masiello, A Weber, and JW Nibler. 2006. “Coherent Raman Spectra of the nu(1) Mode of (BF3)-B-10 and (BF3)-B-11.” *Journal of Molecular Spectroscopy* 237(1):97-103.

Krstic P, RJ Harrison, and BG Sumpter. 2006. “Excited State Quantum-Classical Molecular Dynamics.” *Physica Scripta* T124:101-107.

Krupka KM, HT Schaef, BW Arey, SM Heald, WJ Deutsch, MJ Lindberg, and KJ Cantrell. 2006. “Residual Waste from Hanford Tanks 241-C-203 and 241-C-204: I. Solids Characterization.” *Environmental Science and Technology* 40(12):3749-3754, and supplemental information file.

Lin Y, G Liu, and J Wang. 2006. “Biosensors Fabricated through Electrostatic Assembly of Enzymes/Polyelectrolyte Hybrid Layers on Carbon Nanotubes.” In *Proceedings of Nanotech 2006*, Vol. 2, M Laudon and B Romanowicz, eds., pp. 252-255, NTSI-Nanotech, Boston, Massachusetts.

Luo Q, K Tang, F Yang, A Elias, Y Shen, RJ Moore, R Zhao, KK Hixson, SS Rossie, and RD Smith. 2006. “More Sensitive and Quantitative Proteomic Measurements Using Very Low Flow Rate Porous Silica Monolithic LC Columns with Electrospray Ionization-Mass Spectrometry.” *Journal of Proteome Research* 5(5):1091-1097.

Oehmen CS, T Straatsma, GA Anderson, G Orr, BM Webb-Robertson, RC Taylor, RW Mooney, DJ Baxter, DR Jones, and DA Dixon. 2006. “New Challenges Facing Integrative Biological Science in the Post-Genomic Era.” *Journal of Biological Systems* 14(2):275-293.

Oostrom M, JH Dane, and TW Wietsma. 2006. “A Review of Multidimensional, Multifluid Intermediate-Scale Experiments: Nonaqueous Phase Liquid Dissolution and Enhanced Remediation.” *Vadose Zone Journal* 5:570-598. doi:10.2136/vzj2005.0125

Patwardhan AJ, EF Strittmatter, DG Camp, II, RD Smith, and M Pallavicini. 2006. “Quantitative Proteome Analysis of Breast Cancer Cell Lines using 18O-Labeling and the Accurate Mass and Time Tag Strategy.” *Proteomics* 6(9):2903-2915.

Shumate WJ, DL Mattern, A Jaiswal, DA Dixon, T White, J Burgess, A Honciuc, and RM Metzger. 2006. “Spectroscopy and Rectification of Three Donor-Sigma-Acceptor Compounds, Consisting of a One-Electron Donor (Pyrene or Ferrocene), a One-Electron Acceptor (Perylenebisimide), and a C-19 Swallowtail.” *Journal of Physical Chemistry* 110(23):11146-11159.

Shvartsburg AA, SV Mashkevich, and RD Smith. 2006. “Feasibility of Higher-Order Differential Ion Mobility Separations Using New Asymmetric Waveforms.” *Journal of Physical Chemistry A* 110(8):2663-2673.

Wang CM, J Kwak, D Kim, J Szanyi, R Sharma, S Thevuthasan, and CH Peden. 2006. “Morphological Evolution of $Ba(NO_3)_2$ Supported on an *In Situ* TEM Study.” *Journal of Physical Chemistry B* 110(24):11878-11883. doi:10.1021/jp060235i

Wang X, L Andrews, and J Li. 2006. “Experimental and Theoretical Investigations of Infrared Spectra and Electronic Structures of the $U(OH)_2$, $UO_2(OH)$, and $UO_2(OH)_2$ Molecules.” *Inorganic Chemistry* 45(10):4157-4166.

Whitlow HJ, Y Zhang, CM Wang, DE McCready, T Zhang, and Y Wu. 2006. "Formation of Cobalt Silicide from Filter Metal Vacuum Arc Deposited Films." *Nuclear Instruments and Methods in Physics Research. Section B, Beam Interactions with Materials and Atoms* 247(2):271-278. doi:10.1016/j.nimb.2006.02.016

Woo HK, WB Wang, KC Lau, and LS Wang. 2006. "Low-Temperature Photoelectron Spectroscopy of Aliphatic Dicarboxylate Monoanions, $HO_2C(CH_2)_nCO_2$- (n = 1-10): Hydrogen Bond Induced Cyclization and Strain Energies." *Journal of Physical Chemistry A* 110(25):7801-7805.

Yan P, Y Xiong, B Chen, S Negash, TC Squier, and MU Mayer. 2006. "Fluorophore-Assisted Light Inactivation of Calmodulin Involves Singlet-Oxygen Mediated Cross-Linking and Methionine Oxidation." *Biochemistry* 45(15):4736-4748. doi:10.1021/bi052395a

Yang F, DL Stenoien, EF Strittmatter, J Wang, L Ding, MS Lipton, ME Monroe, CD Nicora, MA Gritsenko, K Tang, R Fang, JN Adkins, DG Camp, II, DJ Chen, and RD Smith. 2006. "Phosphoproteome Profiling of Human Skin Fibroplast Cells in Response to Low- and High-Dose Irradiation." *Journal of Proteome Research* 5(5):1252-1260.

Zhao HB, RG Tonkyn, SE Barlow, BE Koel, and CHF Peden. 2006. "Catalytic Oxidation of HCN over a 0.5% Pt/Al_20_3 Catalyst." *Applied Catalysis B-Environmental* 65(3-4):282-290.

Zubarev DY, AI Boldyrev, X Li, and LS Wang. 2006. "Observation of Triatomic Species with Conflicting Aromaticity: $AlSi_{2-}$ and $AlGe_{2-}$." *Journal of Physical Chemistry B* 110(20):9743-9746.

Zubarev DY, J Li, LS Wang, and AI Boldyrev. 2006. "Theoretical Probing of Deltahedral Closo-AuroBoranes $BxAux2^-$(x = 5-12)." *Inorganic Chemistry* 45(14):5269-5271.

Presentations

During this reporting period, EMSL staff presented on research performed at the user facility at the following meetings or locations.

- 54th ASMS Conference on Mass Spectrometry
- Ohio State Spectroscopy Symposium
- Conference on Lasers and Electro Optics
- Global Change Education Program
- SRI Poster Session, Richland, Washington
- American Geophysical Union Joint Assembly
- Scientific Discovery through Advanced Computing Program (SciDAC)
- Spectral Signatures of Molecular Dynamics Symposium/International Symposium on Molecular Spectroscopy
- The Sixth Annual HP-Cast Meeting
- MSCF Operations Hallway Presentation, Richland, Washington

Patents

U.S. Patent 6,989,674 for the "Advanced Slow-Magic Angle Spinning Probe for Magnetic Resonance Imaging and Spectroscopy" was issued on January 24, 2006, to RA Wind, JZ Hu, KR Minard, and DN Rommereim.

Journal Covers

LS Wang, EMSL user from PNNL, and collaborators have uncovered a class of gold atom clusters that are the first known metallic hollow equivalents of the famous hollow carbon fullerenes known as buckyballs. This research has so far led to stories in several journals and websites, including *Chemical & Engineering News*; the *Seattle Post-Intelligencer*; *Chemistry World*, which is published by the Royal Society of Chemistry in the United Kingdom; and *Nanotechwire*. This work was also featured on the cover of the May 23, 2006, issue of the *Proceedings of the National Academy of Science*.

Cover of the May 23, 2006, issue of the *Proceedings of the National Academy of Science*.